

Figure 1. (a) Normal mouse axial view of normal spleen; (b) 3D reconstructions of the mouse abdomen; (c) 3D coronal view of the spleen

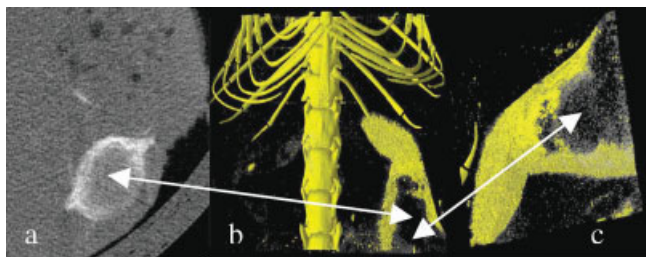


Figure 2. (a) NUDE mouse axial view of tumor in the spleen; (b) and (c) 3D reconstructions of the abdomen and tumor in the spleen

The scanner is equipped with an x-ray micro focus tube with 5 μm focal spot size and operates at 20–100 kV/0–250 μA . A special x-ray camera is based on 10 megapixels rotated around the animal. CT acquisitions at 50 kV and 200 μA were achieved in 40 min to obtain 3D CT images at 18 μm spatial resolution.

Two control Balb/c mice of 23.2 g and two NUDE mice bearing spleen tumor and liver metastasis (weight 17.2 g) were examined. The animals were lying supine on a bed under gas anesthesia (isoflurane) and oxygen 0.5 L/min. All the animals were injected intravenously in the tail vein with 20 mL/kg of Fenestra LC contrast agent, (Alerion Biomedical, San Diego, CA, USA) (3). CT scanning was performed 2 h after injection.

Results: Spleen was clearly visualized by x-ray micro-CT. Figure 1 shows the results of scanning the abdomen area of a healthy live Balb/c mouse: (a) shows a 2D image of the spleen and (b) and (c) show 3D reconstructions of the mouse abdomen and of the spleen, respectively. Figure 2(a) illustrates a spleen image of an abnormal mouse and Fig. 2(b) and (c) show the 3D reconstructions of the tumor in the spleen.

Conclusion: The use of Fenestra LC contrast agent allowed the visualization of the spleen in mice using x-ray micro-CT imaging. The increase in the contrast in the spleen allows automated 3D segmentation and analysis.

References

1. De Clerck NM, Van Dyck D, Postnov AA. Non-invasive high resolution μCT of the inner structure of living animals. *Microsc. Anal.* 2003; **81**: 13–15.
2. Postnov AA, Van Dyck D, Saveliev S, Saso A, De Clerck. Definition of local density in biological calcified tissues using x-ray micro-tomography. *Progress in biomedical optics and imaging. Proc. SPIE* 2002; **3**: 749–755.
3. <http://www.alerionbio.com>.

CMR 2005: 12.02

Micro-CT and micro-DSA of small animal models of disease using iodinated conventional and blood pool contrast agents

C. Badea, L. Hedlund, M. Lin, J. Boslego and G.A. Johnson

Center for In Vivo Microscopy, Duke University Medical Center, Durham, NC, USA

Rationale and Objectives: The availability of genetically manipulated mice has driven biology/drug discovery researchers to confront a smaller and smaller world and to expand the capabilities of imaging systems to accommodate small animals. The amazing array of models of human disease that is now available in mice, for instance, has motivated us to develop new tools to image these very small creatures, *in vivo*, at resolutions that would reveal the smallest details of their organ systems. For *in vivo* studies, we must not only confront the small size of these animals, but also the extremely fast pace of their lives! For these reasons, we have constructed x-ray-based imaging systems (micro-CT, micro-DSA), a microliter power injector, animal support systems and imaging schemes for live mice and rats to achieve resolutions of 50–100 μm pixels with time resolutions of 5–10 ms. Using these new capabilities, we have studied, *in vivo*, a mouse model of heart failure, a rat lung transplant model and also, in rats, vascularization of implanted tumors and coronary artery perfusion.

Methods: We constructed a micro-CT/micro-DSA system that has a high photon fluence rate and integrated motion control (1). Using a stationary tube/detector and a rotating specimen, the geometric blur can be minimized, giving a net usable flux increase at the detector of nearly 250 times higher than with commercial micro-CT systems. For *in vivo* studies, motion is minimized for any single projection with < 10 ms exposures that are synchronized to both cardiac and breathing cycles and to contrast injections. We developed a power, micro-injector that reproducibly delivers as little as 6 μL (about 1% of the blood volume for a mouse) in about 6 ms. We used both a conventional clinical contrast agent, Isovue[®]-370 (Bracco Diagnostics, Princeton, NJ, USA), and a new iodinated blood pool contrast agent, Fenestra[™] VC (Alerion Biomedical, San Diego, CA, USA). Injection routes used included the carotid artery and jugular and tail veins.

Results and Conclusions: Our micro-CT system produced the first *in vivo*, cine, micro-CT of the heart in mice (2) with isotropic spatial resolution (100 μm) and with a temporal resolution of 10 ms. With a constant infusion (1 mL/h) of Isovue, the maximum difference achieved between blood and the myocardium in mouse was \sim 250 HU, whereas after a single injection of Fenestra (0.5 mL per 25 g) this difference was \sim 500 HU. The blood-pool agent provided sufficient contrast for several hours and yielded exquisite micro-CT imaging of the vasculature architecture and cardiac function. For example, using micro-CT and Fenestra, we have characterized both cardiac structure and function (ejection fraction, cardiac output) in a mouse model of heart failure (MLP deficient). Combined micro-CT/micro-DSA studies are being used to evaluate longitudinally pulmonary ventilation and perfusion in a rat lung transplant model. Micro-DSA is being used to visualize coronary arteries in rodents. Both micro-CT and micro-DSA, in conjunction with conventional and blood-pool contrast agents, can play an important role in the analysis of small animal models of disease and in structural and functional phenotyping of rodents.

References

1. Badea CT, Hedlund LW, Johnson GA. Micro-CT with respiratory and cardiac gating. *Med. Phys.* 2004; **31**: 3324–3329.
2. Badea C, Fubara B, Hedlund L, Johnson G. 4D micro-CT of the mouse heart. *Mol. Imaging* in press.

CMR 2005: 12.03

Phage display screening for peptides targeting the amyloid peptide A β_{1-42} for molecular imaging of the senile plaques in Alzheimer disease

C. Burtea,¹ L. Larbanoix,¹ S. Laurent,¹ G. Toubeau,² L. Vander Elst¹ and R.N. Muller¹

¹Department of Organic and Biomedical Chemistry, NMR and Molecular Imaging Laboratory, University of Mons-Hainaut, Mons, Belgium

²Laboratory of Histology, University of Mons-Hainaut, Mons, Belgium

Rationale and Objectives: As a neurodegenerative pathology, Alzheimer disease (AD) is the principal cause of dementia in the elderly (before cerebral stroke and Parkinson disease) and the fourth cause of mortality in developed countries (after cardiac diseases, cancer and cerebral stroke). Its diagnosis can only be confirmed by autopsy, since the symptomatology is common to other neurodegenerative pathologies. The senile plaques, constituted essentially by the amyloid peptide $A\beta_{1-42}$ ($A\beta_{1-42}$), represent the main morpho-pathological feature of Alzheimer disease. An early and non-invasive diagnosis of this pathology would allow a more efficient treatment and may help to prolong the life expectancy of patients suffering from it.

Molecular imaging is a recent and growing discipline, which could help to differentiate AD from other dementias. We propose to attempt MRI detection of the amyloid plaques by using peptides selected by phage display and subsequently grafted to adequate magnetic reporters.

Methods: To select peptides with high affinity for the senile plaques, a disulfide constrained phage display heptapeptide library (New England Biolabs, The Netherlands) was incubated with $A\beta_{1-42}$ (Bachem, Switzerland), which was immobilized by hydrophobic interactions on a plastic surface. After four rounds of selection, 72 candidate phage clones were arbitrarily isolated for further screening of their affinity for the target. The ELISA tests of affinity highlighted 23 phage clones with an optimal affinity for $A\beta_{1-42}$. Their peptide structure was subsequently determined by analysis of the DNA sequence of the fusion insert, and their dissociation constants (K_d) for the target were estimated with the aim of identifying the most efficient peptides. The best one was obtained by solid-phase synthesis and its K_d was again evaluated after biotinylation.

Results: The peptide sequence analysis of the 23 selected phage clones evidenced a more frequent representation of the amino acids Leu, Pro, His and Phe. With the exception of His, these amino acids are hydrophobic. This observation shows the importance of hydrophobic interactions with the target molecule. Concerning the amino acid representation in the peptide structures, the hydrophobic amino acids frequently occupy the first positions whereas Asn and Gln are well represented (~70%) in the seventh position of the insert. The K_d of the 23 selected phage clones ranged from 2.2×10^{-10} to 2.0×10^{-9} M.

Conclusion: The peptide with the most important K_d was selected for further evaluation and *in vivo* detection of the senile plaques in AD by MRI; it will be linked to optimal paramagnetic and superparamagnetic reporters and tested with *in vivo* models.

CMR 2005: 12.04

Stealthy magnetophages, a new tool for molecular imaging

J. Segers, C. Laumonier, S. Laurent, L. Vander Elst and R. N. Muller

Department of Organic and Biomedical Chemistry, NMR and Molecular Imaging Laboratory, University of Mons-Hainaut, Mons, Belgium

Rationale and Objectives: Phage display is a powerful tool in the context of molecular imaging. This technique allows one to select, from a heterogeneous mixture of bacteriophages, each displaying a different peptide on its proteic wall, a vector that is subsequently coupled to a 'contrastophore', i.e. USPIO for MRI. In a previous study (1), we developed the concept of magnetophages, obtained by direct coupling of USPIO to phages isolated after the phage display procedures. We showed that magnetophages can be used as *in vitro* molecular imaging contrast agents (MICAs). However, *in vivo* they are taken up by the phagocytic cells of the reticulo-endothelial system (RES), particularly in the liver. This capture makes magnetophages unavailable to interact

with the target in the context of molecular imaging. Therefore, 'stealthy magnetophages' escaping the RES and showing a prolonged circulation time are suitable.

Methods: Stealthy magnetophages were obtained by covalent coupling of PEGylated USPIO to the amino groups of the proteins of the phage wall. Stealthy magnetophages and non-stealthy magnetophages (i.e. non-PEGylated USPIO), specific or not to the apoptotic marker phosphatidylserine (PS), were injected into anesthetized control male mice and into mice with an apoptotic liver. MRI images were acquired at 4.7 T (Avance 200 system, Bruker, Karlsruhe, Germany) using a T_2 -weighted spin-echo sequence ($TR/TE = 2000/20$ ms, $NE = 4$, matrix 128×128 , slice thickness = 2.5 mm, $FOV = 6$ cm). Intensities of regions of interest (ROI) defined in the liver were measured. Analysis of the images was based on the relative enhancement of the signal (RE) with respect to the pre-contrast image.

Results: Non-stealthy magnetophages, specific or not to PS, induce the RE decrease (Fig. 1), due to their nonspecific internalization by the Kupffer cells of the apoptotic and healthy livers. In contrast, Fig. 2 shows a decrease in RE only in the mice with apoptotic livers. This is conceivably correlated with the specific accumulation of stealthy magnetophages in apoptotic livers and not in healthy ones.

Conclusion: Stealthy magnetophages specific to PS can label apoptotic liver. They are invisible to the RES and can therefore be vectorized to their target. These original systems can thus be used as contrast agents for *in vivo* molecular imaging.

Reference

- Segers J, et al., *Proc. Int. Soc. Magn. Reson. Med.* 2004; **11**: 1710.

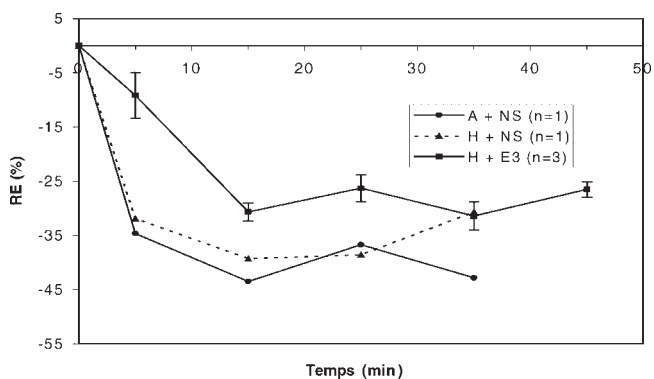


Figure 1. Nonspecific magnetophages (NS) and magnetophages specific to PS (E3) injected into healthy (H) and apoptotic livers (A)

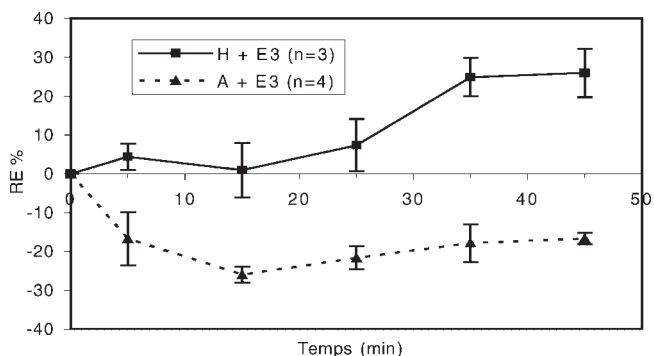


Figure 2. Injection of stealth magnetophages specific to PS (E3) in apoptotic (A) and healthy livers (H)